SAPIENZA
UNIVERSITÀ DI ROMA

FACOLTÀ DI INGEGNERIA DELL'INFORMAZIONE, INFORMATICA E STATISTICA

LOCOMOTION AND HAPTIC INTERFACES FOR VR EXPLORATION

Vibration Suppression Design for Virtual Compliance Control in Bilateral Teleoperation

Professor

Alessandro De Luca

Students

Edoardo Ghini

Gianluca Cerilli

Giuseppe L'Erario

Academic Year 2017/2018

Contents

Introduction

Teleoperation extends the human capability to manipulating objects remotely. An important aspect deals with necessity to obtain, on operator side, similar condition as those at the remote location, in other words, a proper feedback.

A bilateral system is composed by a joystick, called *master*, on the human side, connected to a *slave* on the environment side.

The human imposes a force on the master, that results in a displacement. This displacement is then transmitted to the slave. On the other side, the slave has a force sensor used to "send back" to the master the reflection forces at the environment side. For these reasons we can call it *bilateral teleoperation*.

Two important goals of the teleoperation are [1]:

- **Stability** of the closed loop system irrespective to the behavior of the human and the environment;
- **Transparency** of the teleoperation task: we want forces and displacements be the same on the two sides of the system.

Stability of the system can be ruined by unwanted disturbance, internal and external:

- **Internal disturbance**, due to the uncertainties in modeling of the system;
- **External disturbance**, such as unexpected input contaminated with vibration noise from both sides og the system.

This report deals with the development of a controller able to suppress the vibration and unwanted inputs in a bilateral control system [2].

In this work we investigate the concept of *virtual* spring-damper system with an additional inertia. This concept comes from the design of shock absorbers used in vehicle suspension (which is composed by a spring and damper), and is usually applied in bilateral control system for *soft manipulation*. The disturbance suppression performances depends on the value of these virtual parameters, determined from the desired cut-off frequencies.

The report is organized as follow: in the first part we model the inertia-spring-damper system, analyzing the proposed control and the hybrid matrix. Then is the described the virtual parameter selection process. Finally, we present the results obtained in the simulations, performed with Matlab and Simulink.

1 System Modeling

Nomenclature

- J_m = inertia of the master, kg m^2;
- J_s = inertia of the slave, kg m^2;
- J_{mv} = virtual inertia of the master, kg m^2;
- J_{sv} = virtual inertia of the slave, kg m^2;
- B_v = virtual damping of the system, $\frac{\text{N m}}{\text{rad/s}}$;
- K_v = virtual spring of the system, $\frac{\text{N m}}{\text{rad}}$;
- τ_m = master torque, N m;
- θ_m = master displacement, rad;
- τ_s = slave torque, N m;
- θ_s = slave displacement, rad;

1.1 Modeling

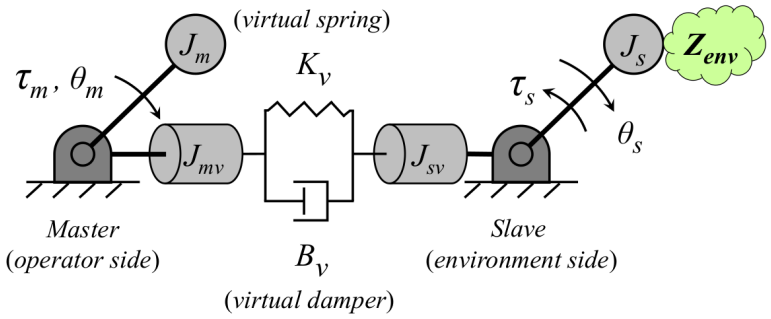

Figure 1: Spring-damper-inertia system with virtual parameters.

The inertia-spring-damper system is shown in Fig.1: the master and the slave have the real inertia J_m and J_s and the virtual ones J_{mv} and J_{sv}. Master and slave are interconnected with the virtual damper B_v and the virtual spring K_v.

The dynamic equations of the system are:

$$(J_m + J_{mv})\ddot{\theta}_m + B_v(\dot{\theta}_m - \dot{\theta}_s) + K_v(\theta_m - \theta_s) = \tau_{ext,m} \tag{1}$$

$$(J_s + J_{sv})\ddot{\theta}_s + B_v(\dot{\theta}_s - \dot{\theta}_m) + K_v(\theta_s - \theta_m) = -\tau_{ext,s} \tag{2}$$

where $\tau_{ext,m} = \tau_h + \tau_{dis,m}$ and $\tau_{ext,s} = \tau_{env} + \tau_{dis,s}$.

The operator (in blue in fig.2) wants to achieve a desired postion θ_d. We can model this behavior as a simple controller $\tau_h = K_h(\theta_d - \theta_m)$.

For the sake of simplicity $\tau_m = \tau_{ext,m}$ and $\tau_s = \tau_{ext,s}$.

Dynamic equations in frequency domain are:

$$(J_m + J_{mv})s^2\theta_m + (B_v s + K_v)(\theta_m - \theta_s) = \tau_m \tag{3}$$

$$(J_s + J_{sv})s^2\theta_s + (B_v s + K_v)(\theta_s - \theta_m) = -\tau_s \tag{4}$$

The virtual parameters are considered elements of the controller. For this aim the equations above are rearranged:

$$J_m s^2\theta_m = \tau_m - (B_v s + K_v)(\theta_m - \theta_s) - J_{mv}s^2\theta_m \tag{5}$$

$$J_s s^2\theta_s = -\tau_s - (B_v s + K_v)(\theta_s - \theta_m) - J_{sv}s^2\theta_s \tag{6}$$

$$\tag{7}$$

where the external torques are action and reaction forces of the human and the environment.

The block diagram of the proposed control system is constructed as shown in Fig.2[1].

A bilateral control can be represented by a 2x2 matrix, called *hybrid matrix*:

$$\begin{bmatrix} \tau_m \\ \theta_s \end{bmatrix} = \begin{bmatrix} H_{11} & H_{12} \\ H_{21} & H_{22} \end{bmatrix} \begin{bmatrix} \theta_m \\ -\tau_s \end{bmatrix} \tag{8}$$

and every H_{ij} is an hybrid parameter.

[1]Delay time in communication channel is not considered in the reference paper [2].

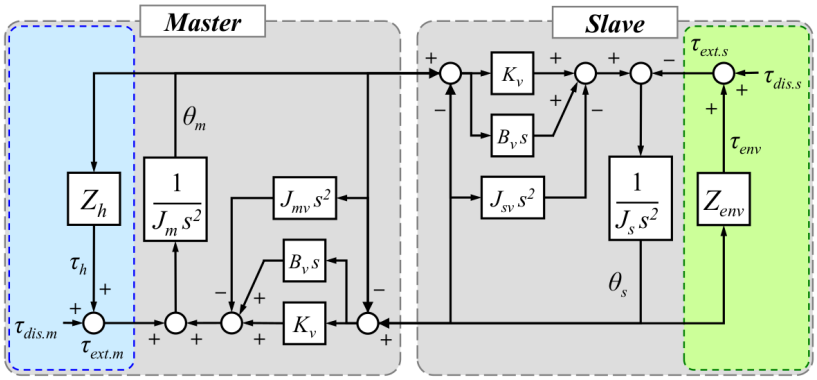

Figure 2: Block diagram of the bilateral control system. The *blue* and the *green* parts of the diagram represent respectively the human and the environment. The human, trying to achieve a desired position θ_d, acts as a simple controller that corrects the position error $e = \theta_d - \theta_m$.

In particular:

$$H_{11} = \frac{1}{Z_s}[Z_m Z_s - (B_v s + K_v)^2] \tag{9}$$

$$H_{12} = -\frac{1}{Z_s}[B_v s + K_v] \tag{10}$$

$$H_{21} = \frac{1}{Z_s}[B_v s + K_v] \tag{11}$$

$$H_{22} = \frac{1}{Z_s} \tag{12}$$

where:

$$Z_m = (J_m + J_{mv})s^2 + B_v s + K_v \tag{13}$$

$$Z_s = (J_s + J_{sv})s^2 + B_v s + K_v \tag{14}$$

The system should achieve two conditions:

- the position of both sides should be the same;
- the law of action-reaction should hold;

represented by the *transparency condition*:

$$\tau_m = \tau_s \tag{15}$$

$$\theta_m = \theta_s \tag{16}$$

It is expressed in terms of transmitted impedance Z_t, which is transferred to the human, and environment impedance Z_{env}:

$$\frac{\tau_m}{\theta_m} = Z_t = Z_{env} = \frac{\tau_s}{\theta_s} \tag{17}$$

The relationship between the transmitted and environment impedance comes from the hybrid matrix of (8):

$$Z_t = \big(\frac{-H_{12}H_{21}}{1 + H_{22}Z_{env}}\big)Z_{env} + H_{11} \tag{18}$$

and, to achieve the perfect transparency condition shown in (17), the hybrid parameters should be derived as:

$$\begin{bmatrix} \tau_m \\ \theta_s \end{bmatrix} = \begin{bmatrix} 0 & -1 \\ 1 & 0 \end{bmatrix} \begin{bmatrix} \theta_m \\ -\tau_s \end{bmatrix} \tag{19}$$

The performances of a teleoperation are evaluated in *free* and *contact* motion. For free motion the external torque on the slave is usually equal to zero, and hence the only parameters affecting the transparency are H_{11} and H_{21}. For contact motion, instead, all the hybrid parameters affect the performance.

1.2 Parameter selection and design

The system is assumed to be disturbed by external vibration noise from the environment. We want to know how the slave position is affected by the external noise. This analysis can be achieved inspecting the hybrid parameter H_{22}, representing how the slave position responds to external torque:

$$\frac{\theta_s}{\tau_{ext}} = \frac{1}{(J_s + J_{sv})s^2 + B_v s + K_v} \tag{20}$$

The virtual parameter in (20) are determined from the second-order characteristic equation of the system:

$$(s + g_1)(s + g_2) = 0 \tag{21}$$

where the poles g_1 and g_2 represent the cut-off frequencies of the system for disturbance suppression purpose.

We can determine the virtual parameters comparing the characteristic equation of (20) with (21).

The operator should feel the reflecting force from the environment vividly. Assuming for a moment we do not care about the vibration suppression, for the proposed control

the system can achieve a large transparency with high spring stiffness K_v and a damping $B_v \to 0$.

It is clear that the value of spring stiffness K_v has an important influence on the transparency of the system: we want to choose it beforehand and the other virtual parameters will be calculated accordingly. The virtual damping coefficient B_v:

$$\frac{B_v}{K_v} = \frac{g_1 + g_2}{g_1 \cdot g_2} \quad \Rightarrow \quad B_v = \frac{g_1 + g_2}{g_1 \cdot g_2} K_v \tag{22}$$

and, in the same fashion, the virtual inertia J_{sv}:

$$J_{sv} = \frac{1}{g_1 \cdot g_2} K_v - J_s \tag{23}$$

The spring stiffness, as said before, influences the behavior of the system. Choosing it properly we can obtain:

- **rigid coupling**, with high stiff spring, obtaining an high transparency;
- **spring coupling**, when the value of the stiffness is low.

In other words we can use the spring stiffness to regulate the *compliance* of the system.

2 Simulations

2.1 Chosen parameters

In regards of the simulation scenarios we are deliberately neglecting the critical aspects of the communication between master and slave.

Therefore all the following simulations has been run assuming ideal conditions as an instantaneous and loss-less signal transfer between master and slave subsystems.

Symbol	Parameter	Value	Unit
	Master-Slave system		
J_m	Master Inertia	$5 \cdot 10^{-4}$	$\mathrm{kg} \cdot \mathrm{m}^2$
J_s	Slave Inertia	$5 \cdot 10^{-4}$	$\mathrm{kg} \cdot \mathrm{m}^2$
	Desired cut-off frequencies		
g_1	1^{st} cut-off frequency	$5 \cdot 10^1$	rad/s
g_2	2^{nd} cut-off frequency	$5 \cdot 10^2$	rad/s

Table 1: Parameters adopted in simulations.

The table n.1 describes the parameters chosen such as inertiae and cut-off frequencies, consequently the table n.2 describes the virtual coefficients computed as explained in section 1.2.

Behaviour	K_v	B_v	J_v
Virtual compliance	$20.0 \ \frac{\mathrm{N\ m}}{\mathrm{rad}}$	$4.4 \cdot 10^{-1} \ \frac{\mathrm{N\ m}}{\mathrm{rad/s}}$	$3 \cdot 10^{-4}$ kg m^2
Rigid coupling	$10^2 \ \frac{\mathrm{N\ m}}{\mathrm{rad}}$	$1.5 \cdot 10^{-1} \ \frac{\mathrm{N\ m}}{\mathrm{rad/s}}$	0 kg m^2

Table 2: Sets of chosen virtual parameters.

2.2 Disturbance rejection performances

We consider at first the rigid coupling case, in which, as being said, almost full transparency is achieved between master and slave. The vibrations transmitted by the environment on the slave-side will be felt almost with the same intensity on the master-side whatever would be the vibration frequency.

For this reason, in order to reach better task execution performances we want to reduce the impact of environment vibrations at minimum.

The simulations aims to compare two opposite behaviours: **rigid coupling** and **induced virtual compliance**, achieved through the choice of the desired cut-off frequencies.

Fig.3 describes the frequency response of the function (20) with several virtual parameters sets, defined starting from different spring stiffness values K_v varying from 2.5 $\mathrm{N} \cdot \mathrm{m/rad}$ to 20 $\mathrm{N} \cdot \mathrm{m/rad}$, and the rigid coupling control set.

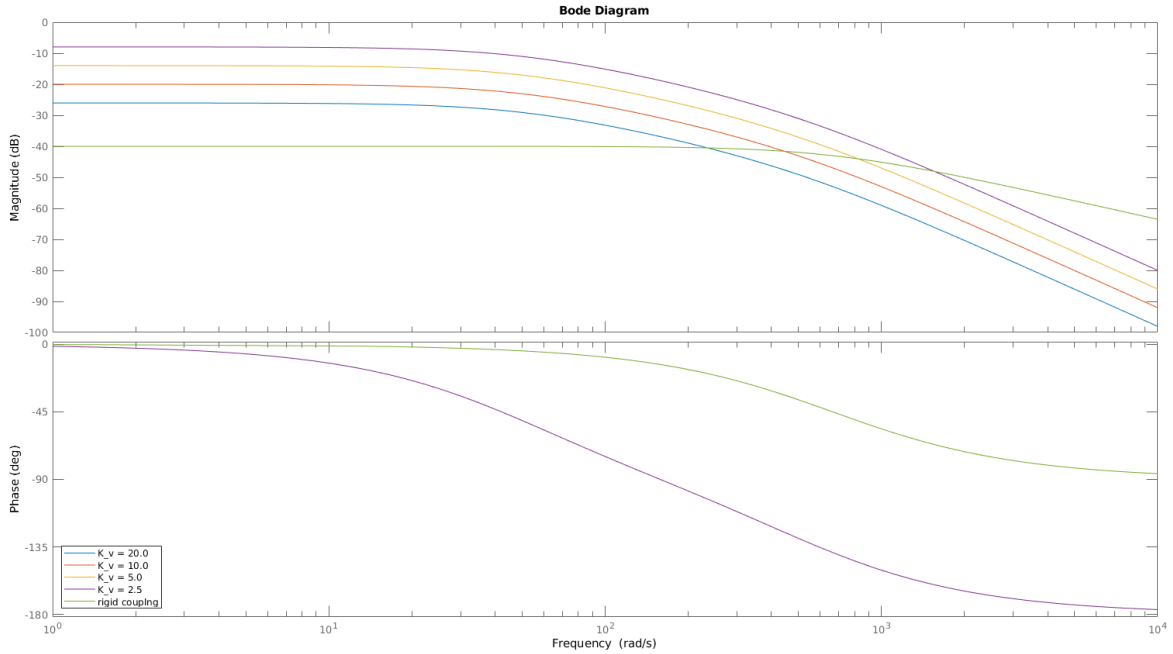

Figure 3: Frequency response relative to H_{22} hybrid parameter.

At low frequencies the signals are preserved in both the rigid coupling and the virtual compliance controls. In particular, the magnitude of the response increases with inverse of the virtual spring stiffness, describing the **compliance** of the system. At high frequencies the disturbance rejection is exerted more effectively by the virtual compliance control: the position response to high frequency external torque is reduced due to the low compliance.

A comparison of the vibration suppression applied on three different input frequencies is interesting, (figs.4) [2]:

- 10 Hz input : in fig.4a is shown how the inputs at lower frequencies are preserved by the **control set 4** (defined by $K_v = 2.5$ N $\cdot$ m/s - purple line). The response is less large as stiffness increases. The phase is almost the same for virtual compliance and rigid coupling controls;

- 10^2 Hz input : as before, the response decreases as the virtual spring stiffness

[2]For the sake of simplicity the different control set are called:

- Control set 1 : defined by $K_v = 20.0$ $\frac{\text{N}\cdot\text{m}}{\text{rad}}$;
- Control set 2 : defined by $K_v = 10.0$ $\frac{\text{N}\cdot\text{m}}{\text{rad}}$;
- Control set 3 : defined by $K_v = 5.0$ $\frac{\text{N}\cdot\text{m}}{\text{rad}}$;
- Control set 4 : defined by $K_v = 2.5$ $\frac{\text{N}\cdot\text{m}}{\text{rad}}$.

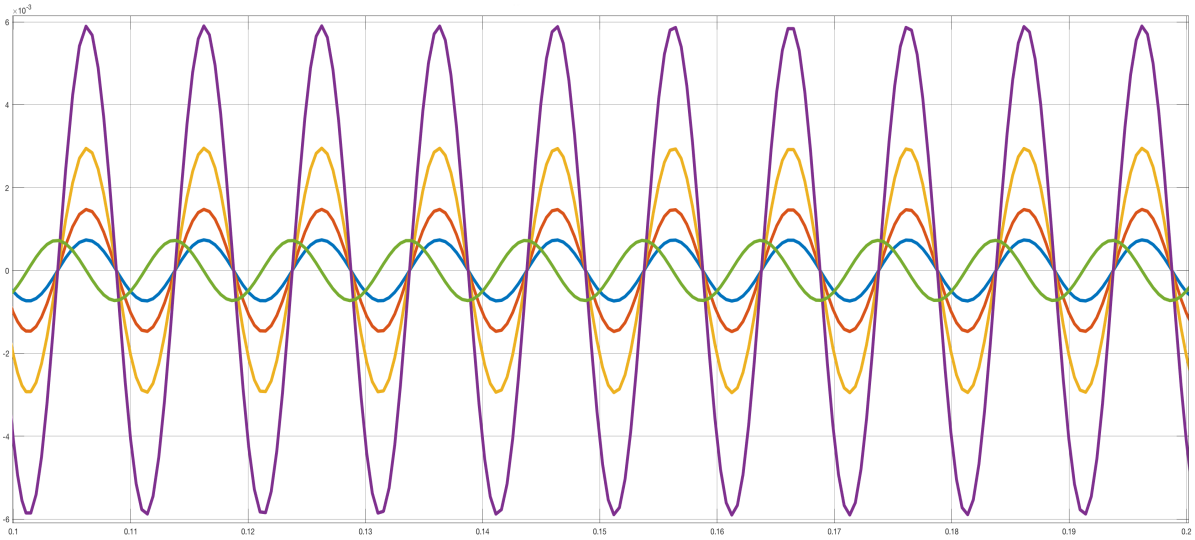

(b) 100 Hz

increase. The difference here is the almost the same response of the **control set 1** ($K_v = 20$ N $\cdot$ m/s - blue line) and the rigid coupling ($K_v = 10^2$ N $\cdot$ m/s - green line), despite the second one is defined by a larger value of stiffness. The phase relative to the **control sets** is delayed respect to the rigid coupling control (fig.4b);

- 10^3 Hz input : at frequencies higher than the cut-off ones, the inputs are dumped more effectively by the **control sets** than the **rigid coupling control**, for which we have larger response (fig.4c).

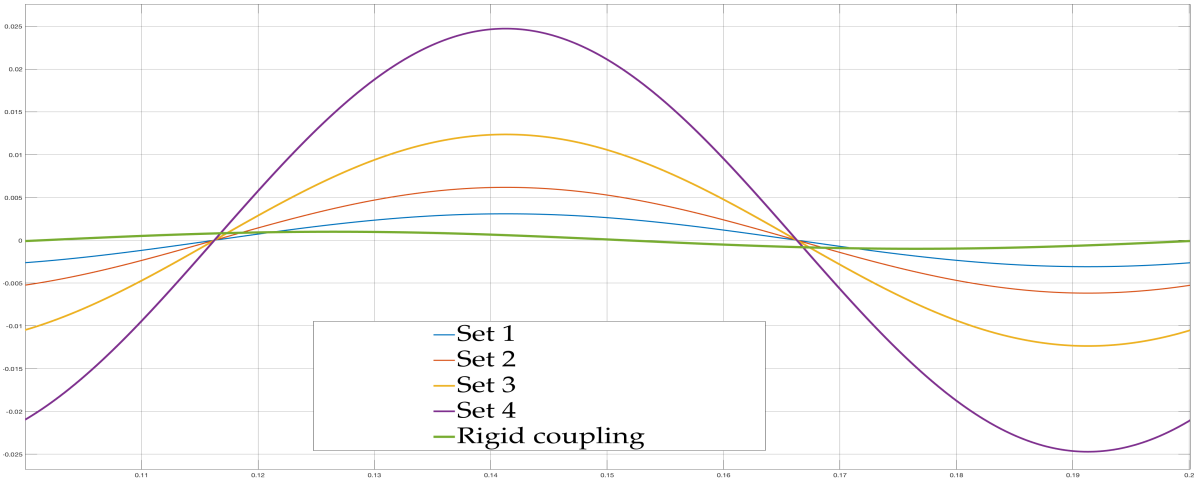

(a) 10 Hz

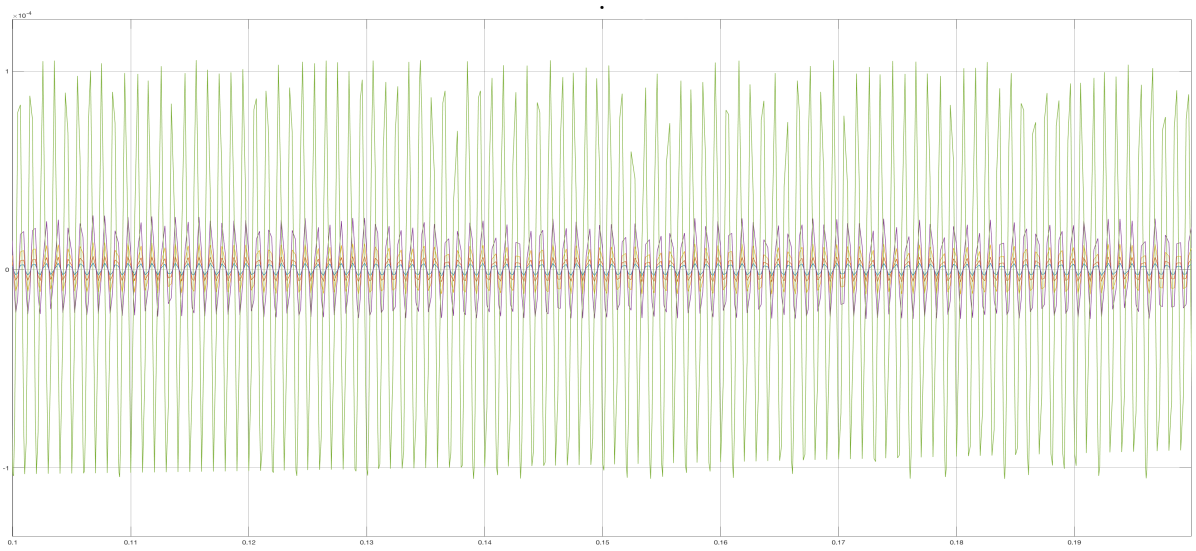

(c) 1000 Hz

Figure 4: Slave position response to a sinusoidal input with three different frequencies.

2.3 Task execution analysis

Simulation setup

The operator is modeled as spring-damper system ($K = 200.0$ N/m and $B = 4.0$ N·s/m). The master-slave system has arms of length equal to 0.1 m.

The environment with which the slave manipulator comes into contact is modeled as:

- free motion: the environment has no stiffness but just a small damping $B_{env} = 0.01 \text{ N} \cdot \text{s/m}$;
- contact motion: the environment has spring stiffness $K_{env} = 100.0$ N/m after a chosen value of displacement, modeling a not totally rigid body.

The simulation are performed with the **control set 4** ($K_v = 20.0 \frac{\text{N m}}{\text{rad}}$, $B_v = 4.4 \cdot 10^{-1} \frac{\text{N m}}{\text{rad/s}}$, $J_v = 3 \cdot 10^{-4}$ kg m^2) and are compared with the **rigid coupling control** ($K_v = 10^2 \frac{\text{N m}}{\text{rad}}$, $B_v = 1.5 \cdot 10^{-1} \frac{\text{N m}}{\text{rad/s}}$, $J_v = 0$ kg m^2).

2.3.1 Free motion with high frequency input

At first, we present an execution in free motion. The slave manages to mirror the master which is moved according to a 0.11 Hz sinusoidal trajectory. Applying both *rigid coupling control* (fig.6a) and *virtual compliance control* (fig.5a) there is almost no task error.

The noise of the system is modeled as a mixture of white noise and sinusoidal oscillations both at frequency of 50 Hz on the slave side.

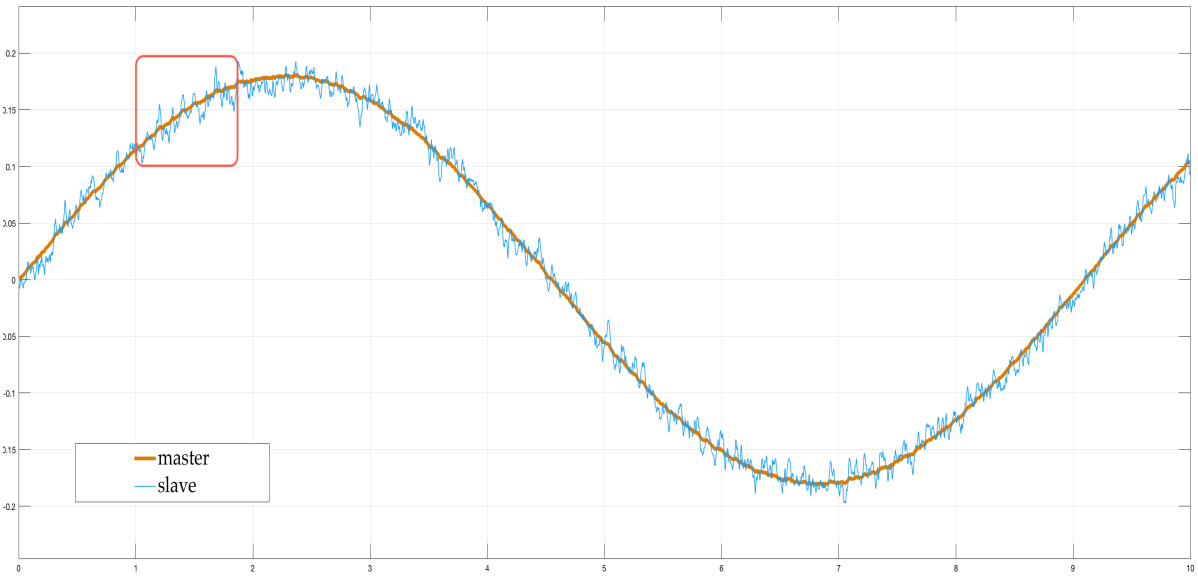

(a) Positions of the master-slave system in free motion - virtual compliance control.

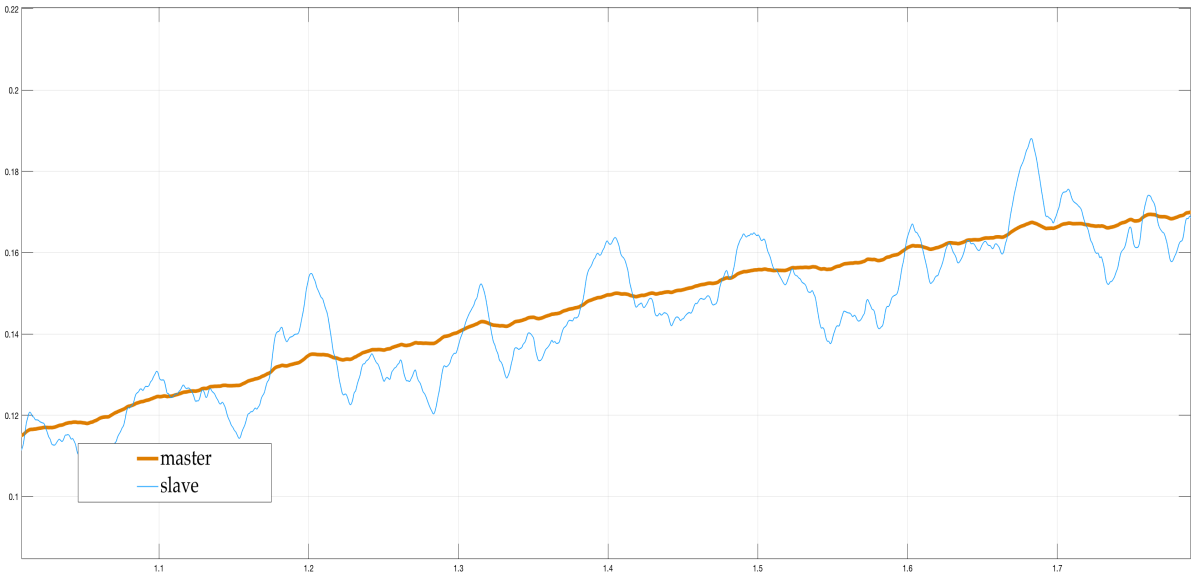

(b) Detail describing the highlighted area in fig.5a

Figure 5: **High** frequency disturbances response - virtual compliance control.

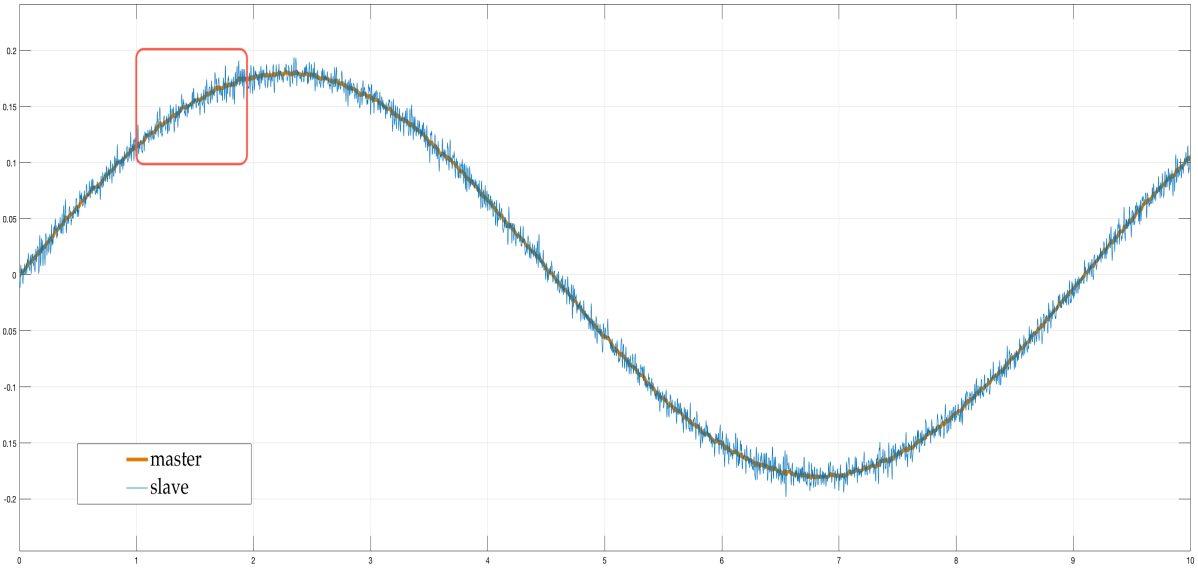

(a) Positions of the master-slave system in free motion - rigid coupling control.

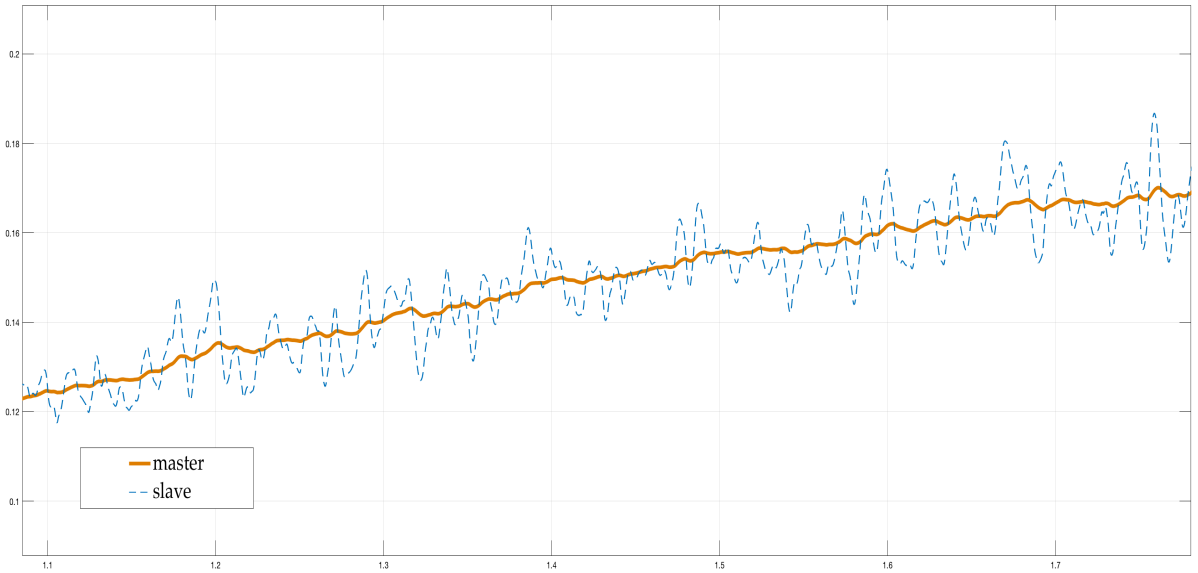

(b) Detail describing the highlighted area in fig.6a.

Figure 6: **High** frequency disturbances response - rigid coupling control.

A comparison between the fig.6b and the fig.5b shows how is the slave response under the two different type of controllers: the response is slower using the virtual compliance control respect to the rigid coupling control. By consequence, the operator "feels" less disturbances.

2.3.2 Free motion with low frequency input

Comparatively, two other simulations have been performed under the same conditions of the previous ones. Here the input frequency is lowered to 20.0 Hz.

Usually, one wants this type of inputs to be detectable, and hence, they should be preserved.

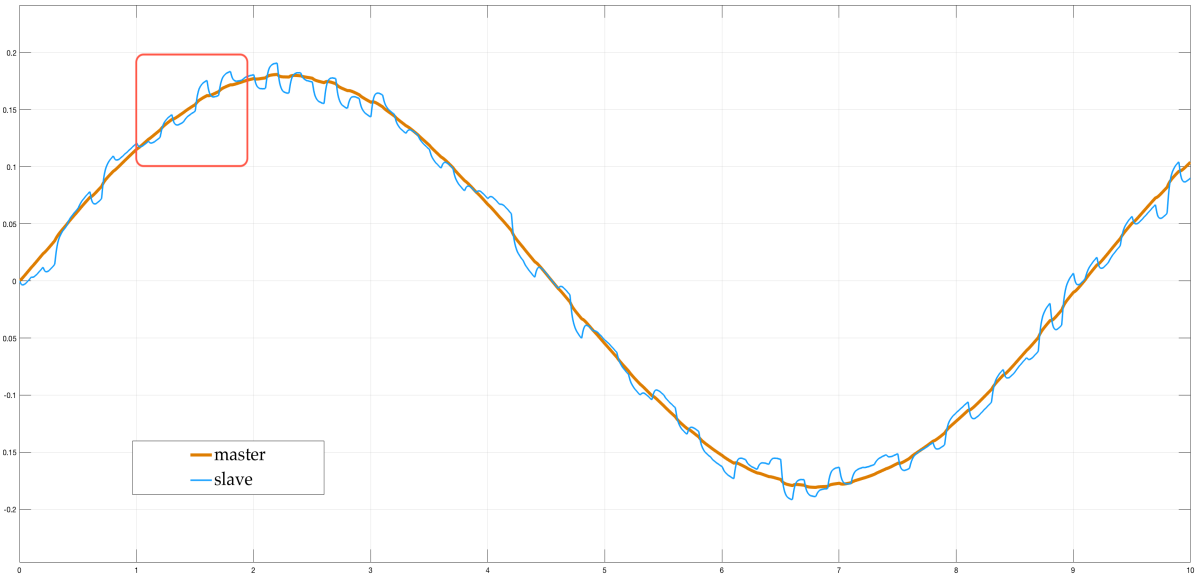

(a) Positions of the master-slave system in free motion - virtual compliance control.

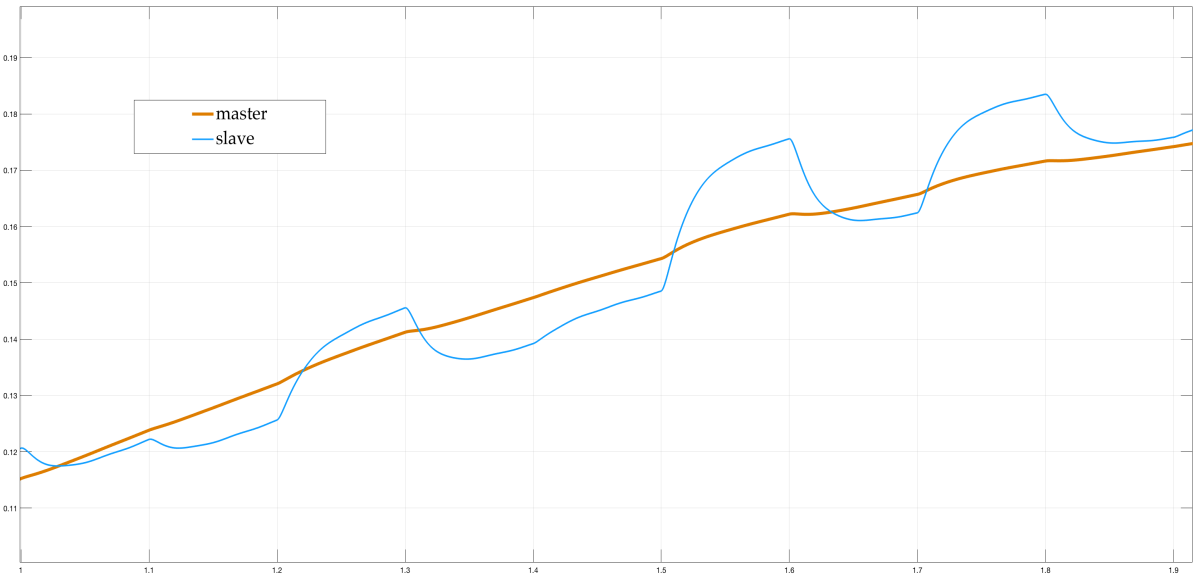

(b) Detail describing the highlighted area in fig.7a

Figure 7: **Low** frequency disturbances response - virtual compliance control.

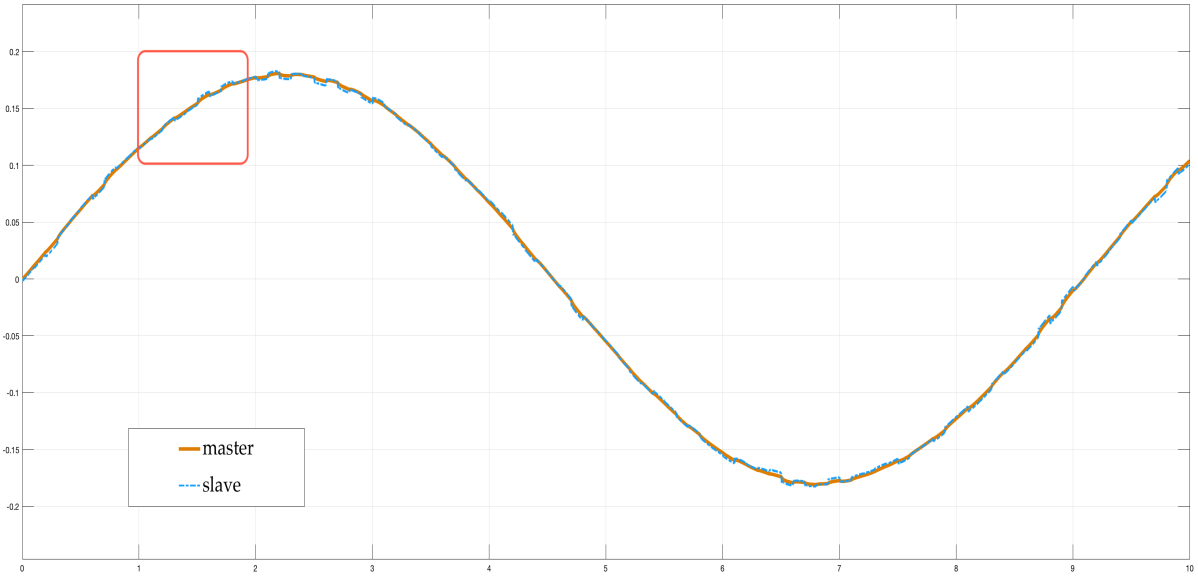

(a) Positions of the master-slave system in free motion - rigid coupling control.

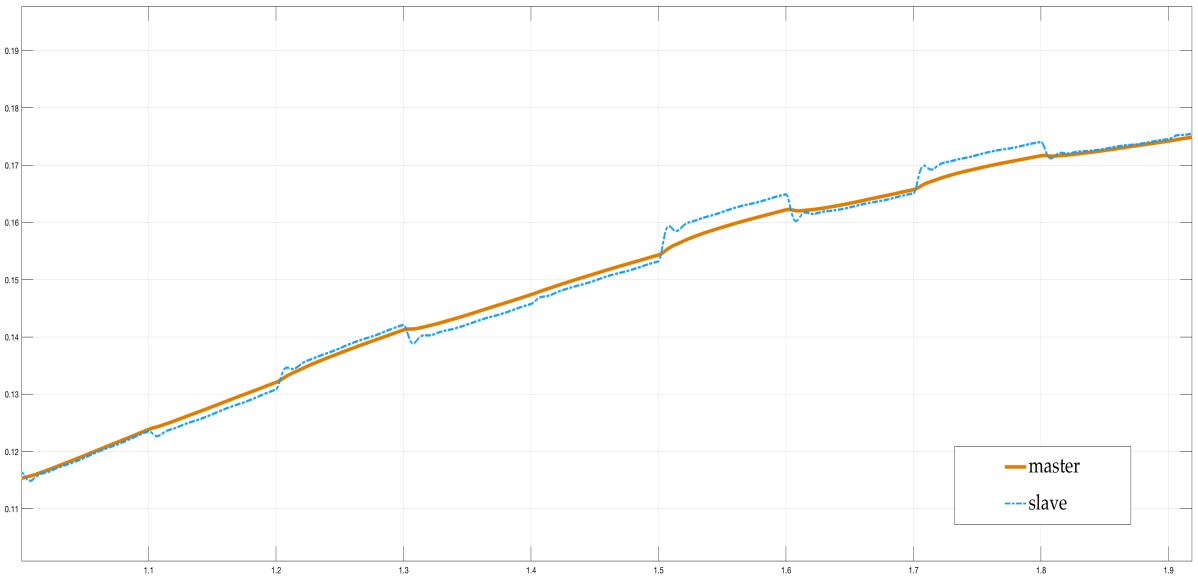

(b) Detail describing the highlighted area in fig.8a

Figure 8: **Low** frequency disturbances response - rigid coupling control.

This phenomenon shows up in fig.8b and fig.7b. Infact the two profiles confirm that *rigid coupling control* cancel out most of the useful information from the signal, while *virtual compliance control* saves the signal information.

2.3.3 Contact motion

In this section the reference trajectory for master is equal to the one used for the simulations in free motion.

The slave, overcoming a certain angle value, is in contact with the environment. This will not allow a perfect tracking by the slave.

The comparison between *virtual compliance control* and *rigid coupling control* in presence of a contact with the environment can be deduced by the differences in **magnitude** of the arrows drawn in the fig.9 and fig.10.

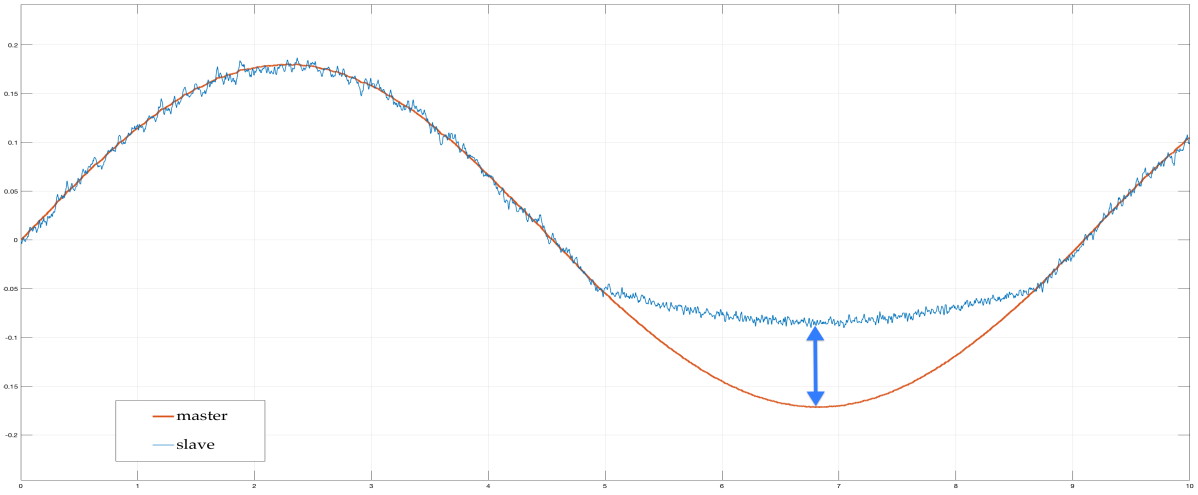

(a) Position assumed during trajectory tracking.

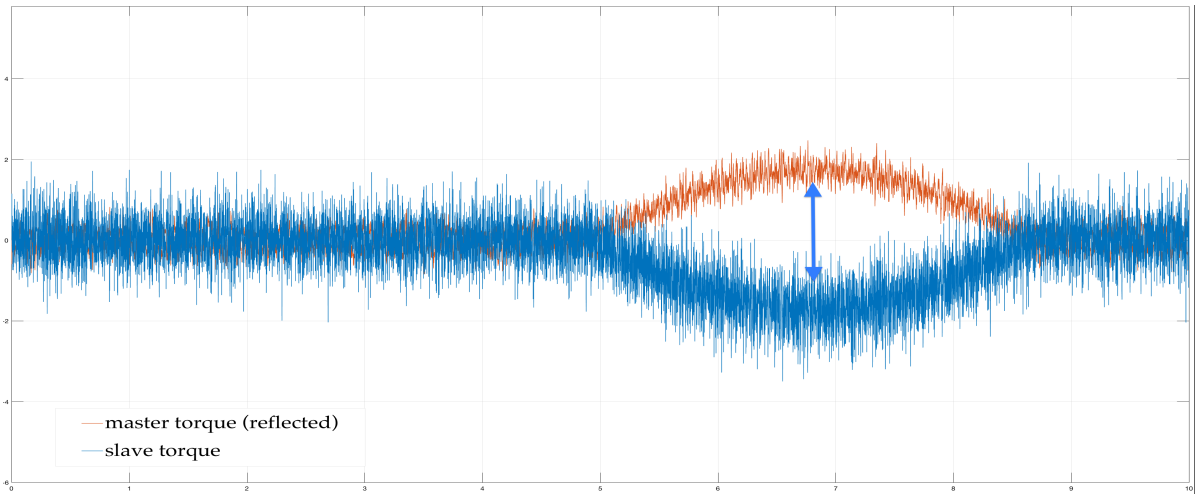

(b) Torques exerted over time.

Figure 9: Contact motion simulation - virtual compliance control.

During the contact motion phase, a gap between the master and the slave position emerges. Fig.9a shows as the *virtual compliance control* leads to a larger position error then the *rigid coupling control* (fig.10a): with high spring stiffness value the gap is closer.

From the point of view of the torque exerted, the proposed control (fig.9b) performs more efficiently than *rigid coupling coupling* (fig.10b), suppressing the high frequency noise from the environment to the master side.

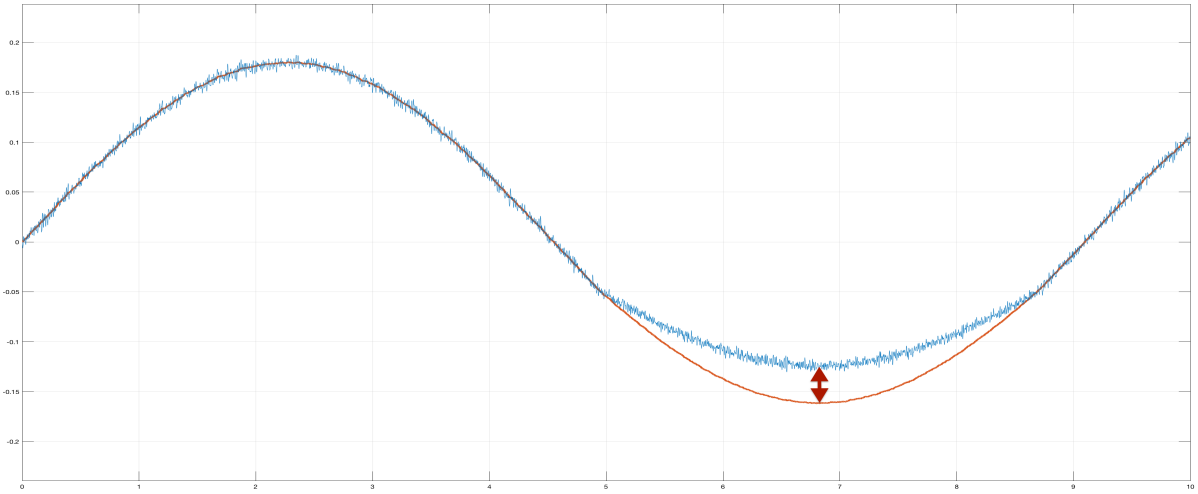

(a) Angular position assumed during trajectory tracking.

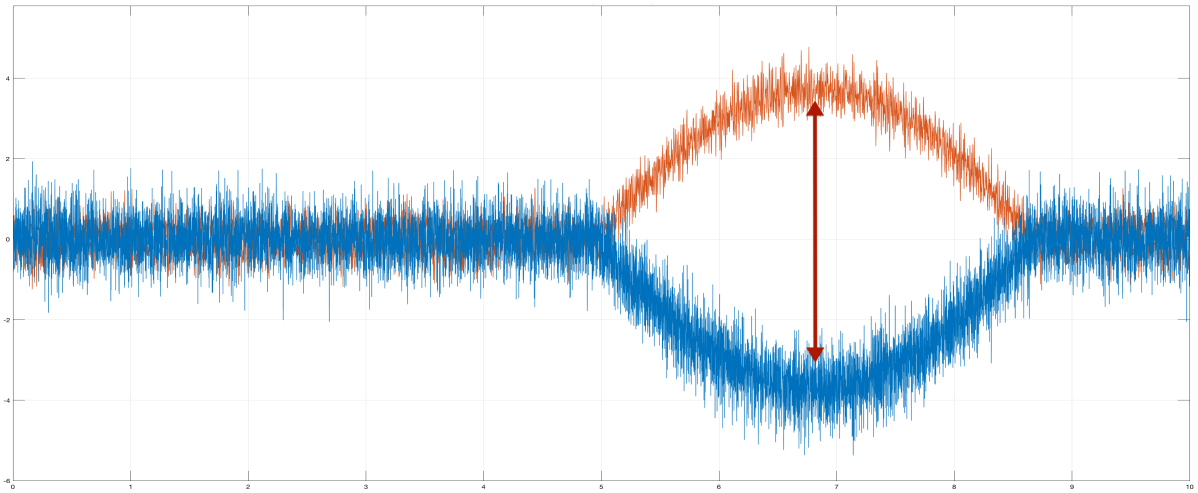

(b) Torques exerted over time

Figure 10: Rigid coupling simulation in *contact* with the environment

3 Conclusions

Vibration suppression in the contest of bilateral teleoperation is an open issue.

The proposed solution is based on a virtual spring-damper system with additional inertia. The spring stiffness and the cut-off frequencies are chosen according to the system requirements.

To summarize, when the virtual stiffness has been fixed, the other virtual parameters could be calculated from the equations in order to obtain the desired cut-off frequencies.

The tracking error in *free motion* is almost the same, using both **virtual compliance control** and **rigid coupling control**. However,the proposed controller shows promising results, since it preserves the useful (*low*) frequency inputs and reject the noisy ones (*high*).

In *contact motion* the usage of the proposed controller leads to a position gap between master and slave and hence can be applied only to tasks that involve the handling of *soft* materials.

References

[1] P. F. Hokayem and M. W. Spong, "Bilateral teleoperation: An historical survey," *Automatica*, vol. 42, no. 12, pp. 2035–2057, 2006.

[2] C. Trakarnchaiyo and A. H. S. Abeykoon, "Vibration suppression design for virtual compliance control in bilateral teleoperation," in *Control and Robotics Engineering (ICCRE), 2017 2nd International Conference on*, pp. 57–62, IEEE, 2017.